JEE Journal of Ecological Engineering

Journal of Ecological Engineering, 2025, 26(7), 77–92
https://doi.org/10.12911/22998993/203138
ISSN 2299–8993, License CC-BY 4.0

Received: 2025.03.19
Accepted: 2025.04.30
Published: 2025.05.15

Toxicity changes of chlorfenvinphos using ozone, ultraviolet light-assisted ozonation, photocatalysis and persulfates activated by visible light

Piotr Zawadzki[1]

[1] Central Mining Institute, National Research Institute, Department of Water Protection, Plac Gwarków 1, Katowice, Poland
E-mail: pzawadzki@gig.eu

ABSTRACT

The aim of this study is to determine the toxicity of solutions obtained after the advanced oxidation processes of chlorfenvinphos using ozone (O_3), ultraviolet light-assisted ozonation (O_3/UV) and photocatalysis (TiO_2/UV) as well as persulfates activated by visible light (PS/Vis). Basic technological parameters for improving the environmental safety of treated aqueous solutions polluted with chlorfenvinphos were determined. The model solution prepared based on deionised water and a chlorfenvinphos standard was subjected to various methods of advanced oxidation (O_3; O_3/UV; TiO_2/UV; PS/Vis). The advanced oxidation processes were conducted for up to 45 minutes, and the post-process solution toxicity was subsequently analysed using the embryophyte Lepidium sativum (garden cress) and the bacteria *Aliivibrio fischeri* (MICROTOX® biotest). It was revealed that the PS/Vis process was the most effective for CFVP removal [($C/C_{0[CFVP]}$), mineralisation (%TOC) and biological safety (bioluminescence inhibition, germination index). The toxicity assessment by *Aliivibrio fischeri* and *Lepidium sativum* demonstrated that the reaction mixture subjected to the effects of PS/Vis was within the scale of nontoxicity. The experimental testing showed that optimal process conditions result in the highest efficiency of CFVP degradation and improved biological safety. It was found that the PS/Vis process can be a valuable alternative to O_3, O_3/UV and TiO_2/UV.

Keywords: chlorfenvinphos, persulfates, advanced oxidation, toxicity assessment, MICROTOX®.

INTRODUCTION

Compounds or groups of compounds recognised as priority substances include [(EZ)-2-Chloro-1-(2,4-dichlorophenyl)ethenyl] diethyl phosphate, widely known as chlorfenvinphos (CFVP). Chlorfenvinphos is an organophosphorus insecticide, a category of very toxic environmental pollutants. Technical chlorfenvinphos, composed of a sum of E and Z isomers, contains 90% of this compound (Sosnowska et al., 2013). CFVP is used as an insecticide with minor toxicity towards mammals. Its effects consist in inhibiting the activity of acetylcholinesterase, one of the more important enzymes for the central and peripheral nervous system (Sigurnjak et al., 2020). Chlorfenvinphos exhibits a moderate bioconcentration potential, as indicated by the value of $\log_{KOW}$ = 3.81–4.22 (depending on the isomer). In the case of organic substances with $\log_{KOW}$ below 4.5, it is assumed that the affinity for the lipids of an organism is insufficient to exceed the bioconcentration factor (BCF = 2000). The level of CFVP bioconcentration in plants, which is a ratio of the substance concentration in the organism and the water, is 36.6–661.0 depending on the organism and the conditions (Koranteng et al., 2018).

Conventional wastewater treatment technologies such as coagulation, sedimentation, filtration or biological decomposition are insufficient, as indicated by the presence of CFVP in samples collected from liquid (groundwater, surface water, sea water, wastewater) and solid media (bottoms, sewage sludge) all over the world (Barbieri et al., 2021). The Directive (2013/39/EU 2013) indicates the necessity to develop new technologies for eliminating priority substances and priority hazardous substances. One of the

more interesting methods for priority substance elimination includes advanced oxidation processes (AOPs).

Due to the high investment and operating costs as well as the risk of generating oxidation by-products, the use of AOPs is recommended for the final stage of wastewater treatment (4th or 5th degree of treatment) (Ameta, 2018). The common feature of AOPs involves using the oxidation potential of hydroxyl radicals (•OH). Reactions conducted in the presence of these radicals are non-selective, and the oxidation potential E0 is 2.80 V. Numerous processes that generate •OH are known, such as photocatalysis (TiO_2/UV) or ultraviolet light-assisted ozonation (O_3/UV) (Rayaroth et al., 2023). According to recent literature reports, oxidation by sulfate radicals also draws major interest, as these are characterised by a higher oxidation potential (E^0 = 2.50–3.10 V) than •OH radicals (Honarmandrad et al., 2023).

Sulfate radicals are generated by the effects of various energy sources (e.g. heat, UV light) on initiators such as sodium persulfate ($Na_2S_2O_8$) or following the reactions of transition metal ions (e.g. Fe^{2+}, Co^{2+}). Conventional activation methods based on UV light or heat currently appear very cost-ineffective due to the energy crisis and its consequent rise in the prices of electricity (Delardas and Giannos 2022). It is therefore justified to apply alternative activation methods such as modified AOPs in order to use renewable energy sources, including visible light (Vis). Such modifications also include the use of sugars (e.g. glucose, sucrose) as the source of electrons necessary to activate persulfates. The advantage of using visible light is primarily the availability of an inexpensive and renewable energy source. On the other hand, sugars exhibit no toxic effects on living organisms and cost nearly twice as little as e.g. Fe^{2+} ions (Zawadzki, 2019).

In advanced oxidation processes, it is not only the investment and operating costs or the pollutant degradation efficiency that determine the effectiveness of AOPs. It was revealed that a phenomenon characteristic for advanced oxidation processes is the risk of generating toxic oxidation by-products (Alderete et al. 2021). This occurs e.g. under technical conditions, where sometimes it is impossible (e.g. due to costs) to control the process in order to avoid the generation of oxidation by-products. Oxidation by-product generation may be caused by a high pollutant concentration or an insufficient oxidative dose, a low oxidation potential, and a reduced likelihood of oxidative radical and pollutant molecule collision. Despite the high efficiency of AOPs in degrading numerous pollutants, the oxidation by-products require particular attention, as they are often more toxic and hazardous than the initial compounds (Lellis et al., 2019). It is reported that CFVP by-products include, for example: 2-hydroxy-1-(2,4-dichlorophenyl) vinyl diethyl phosphate; 2,4-dichlorobenzoic acid; dicarboxylic acid; 2,4-dichlorophenol; triethyl phosphate; 4-hydroxybenzoic acid (Roselló-Márquez et al., 2021).

The post-process solution toxicity assessment can be performed based on commercial toxicological biotests, such as: MICROTOX® (bacteria *Aliivibrio fischeri*), DAPHTOXKIT® (crustaceans Daphnia magna) or ARTOXKIT M® (crustaceans *Artemia salina*) (Foszpańczyk et al., 2018). Toxicity tests are also conducted using the freshwater fish Danio rerio (Cabascango et al. 2021) and duckweed Lemna sp. (Growth Inhibition Test) (Foka Wembe et al., 2023). The estrogenic and androgenic activity of intermediate products is also assessed by means of in-vitro YES (Yeast Estrogen Screen) and YAS (Yeast Androgen Screen) tests utilising the yeast Saccharomyces cerevisiae.

As part of this study, the toxicity of post-process solutions was analysed using the bacteria Aliivibrio fischeri (MICROTOX® biotest) and the embryophyte Lepidium sativum (garden cress). The MICROTOX® biotest was selected because of the *Aliivibrio fischeri* bacteria's sensitivity to a broad spectrum of toxic substances and contaminations. Further advantages of the test include: the short time required for analysis, well-defined protocols, repeatability and sensitivity (Rueda-Márquez et al., 2020). The contact of the bacteria with pollutants leads to reactions that result in bioluminescence inhibition (Abbas et al., 2018). Phytotoxicity tests using garden cress were selected, as biological tests utilising plants are recognised in literature as a useful tool for water and wastewater quality control, particularly in cases of potential water reuse for irrigation, e.g. in agriculture (Mahmoudi et al., 2022). The primary advantages of using garden cress include: the broad availability of seeds, the low test cost and the availability of various test parameters (germination rate, stem growth, root growth).

The novelty of this work can be found in the comparative toxicity analysis of post-process solutions obtained following commonly applied

processes, such as O_3, O_3/UV and TiO_2/UV, as well as in the innovative persulfate activation process by means of visible light for degrading a pesticide – chlorfenvinphos. The results of toxicity testing for O_3 (Pandis et al., 2022), O_3/UV (Dong et al., 2022) or TiO_2/UV (Lambropoulou et al., 2017) processes are known. Other methods of chlorfenvinphos treatment are also known, such as electrochemical oxidation (Mora-Gómez et al., 2022) combined with post-process solution toxicity assessment, though available research devotes no attention to processes involving visible light. Nevertheless, little information is currently available on the toxicity of post-process solutions obtained by PS/Vis. Although methods for degradation and toxicity evaluation of pollutants using ozone or titanium(IV) oxide are known, few publications have focused on the toxicity evaluation of the innovative process of visible-light activation of persulfate. In particular, there is a lack of studies on evaluating the toxicity of post-process solutions using persulfate to remove chlorfenvinphos. As the studies show, CFVP is still identified in the environment despite the ban on its use. There is an urgent need for its removal and monitoring, which is well documented, for example by the Directive 2013/39/EU of the European Union. Failure to improve AOPS processes, for example through the toxicity assessments will result in further deepening of this serious environmental problem. Therefore, the primary aim of this paper was to investigate the post-process solution toxicity and to inspect the technological parameters that determine the environmentally safe treatment of chlorfenvinphos-polluted solutions. The work will familiarise the readers with an important source of information on the parameters that influence chlorfenvinphos degradation in various advanced oxidation processes as well as regarding the toxicity of post-process solutions, which constitutes valuable knowledge and will help researchers who tackle similar issues in developing the appropriate treatment plans for industrial wastewater containing pesticides, including chlorfenvinphos.

MATERIALS AND METHODS

Materials

The object of study included model solutions prepared based on deionised water with an added chlorfenvinphos standard (CFVP) with a purity > 95% and a concentration of 50 µg/L. The pesticide concentration is within the range of typical environmental concentration. For example, in Poland, chlorfenvinphos was identified at 32 surface water samples out of 137 measurement points in Silesia (Chief Inspectorate for Environmental Protection 2016). CFVP concentrations ranged up to 47.4 µg/L. Chlorfenvinphos was also identified in Portuguese surface waters at a concentration of 31.6 µg/L (Cerejeira et al., 2003) and offshore waters around England and Wales at a concentration of 30.8 µg/L (Environment Agency, 1997). The serious need to eliminate CFVPs was indicated in the study (Kowalska et al., 2004). It was shown that the concentration of CFVP in influent wastewater from the pesticide plant was more than 1.5 mg/L, whereas in the treated outflow was 65.0 µg/L. Incomplete removal of chlorfenvinphos results in its identification not only in raw or treated wastewater, but also in surface water and other environmental samples around the world. Therefore, 50 µg/L was taken as the typical environmental concentration of CFVP. The CFVP removal was conducted by means of oxidation radicals (sulfate, hydroxyl) initiated by sodium persulfate ($Na_2S_2O_8$) and ozone (O_3). The $Na_2S_2O_8$ purity was ≥ 99%. The photocatalysis process was conducted in the presence of commercial titanium dioxide (TiO_2 P-25) with a purity of 99.5%. The specific surface area of TiO_2 is 35–65 m^2/g. The chemical reagents and materials used during the experiment were produced by Sigma-Aldrich (Poznań, Poland).

Instruments and analytical methods

The analytes were subjected to HPLC chromatographic analysis by means of a Perlan Technologies (Warsaw, Poland) model 1200 UV detector in accordance with PN-EN ISO 11369 (ISO 11369 1997). Where necessary, particulate matter (e.g. of the photocatalysts) was separated from the samples by means of a filtration device through a 0.45 µm cellulose acetate filter (Microlab Scientific Co., Ltd., USA). The chromatographic analysis was preceded by separating the compound by means of solid phase extraction (SPE) in CHROMABOND® C18 ec columns. The total organic carbon was determined by high-temperature combustion with IR detection in accordance with PN-EN 1484:1999 (PN EN 1484 1999).

Advanced oxidation experiments

The oxidation was conducted continuously over a time of up to 45 min. The experimental conditions, i.e. the temperature (T = 295.0 K), atmospheric pressure (p = 1011.0 hPa), reaction vessel volume (V = 0.5 L) and reaction vessel shape (cylindrical borosilicate glass beakers) remained constant during each experiment. The reaction mixture volume was 0.4 L. The pH = 6.0, which is the pH typically found in wastewater, was used as the limiting model reaction. Environmentally and especially in terms of operating costs, it is not justified to lower or increase the pH. The initial CFVP concentration ($C_{0[CFVP]}$) was set to 25–200 µg/L. The ozonation was conducted by means of an Eltom (Warsaw, Poland) ZY-H103 ozonator with a power of 20 W. The ozone dosage was determined at 50–125 mg/L. The TiO_2 dosage was 25–100 mg/L. The oxidation by persulfates (SPS) was conducted using sodium persulfate ($Na_2S_2O_8$) at a concentration of 1–10 mM. The oxidation by $Na_2S_2O_8$ was assisted with a glucose addition at a concentration of 100 mM. The experiments using a UV lamp utilised a Grech (Maao, China) CUV-510 lamp with a power of 10 W (λ = 254 nm). The experiments using a Vis lamp as the source of visible light utilised a Thorlabs Inc. (New Jersey, USA) QTH10/M tungsten lamp with a power of 10 W. The lamp emitted radiation with a wavelength λ = 400–710 nm. All the experiments were conducted independently and repeated thrice. Mean values with standard deviation were used for the data analysis. The CFVP removal efficiency (R) was calculated based on formula (1) (Ahmadi et al., 2020).

$$R = \frac{C_0 - C_t}{C_0} \cdot 100 \quad (1)$$

where: R – removal efficiency [%], C_0 – initial concentration of CFVP [-], C_t – concentration of CFVP at t time [-].

Toxicity measurements

Defining the potential risk related to the toxicity of post-process solutions towards plants and bacteria was the dominant aspect of this work. Living organisms are exposed to chlorfenvinphos when it is directly or indirectly released into the environment. Chlorfenvinphos enters into the surface and ground water as a result of surface runoff from arable land, farmlands or their vicinity. The surface runoff determines the transport of chlorfenvinphos particularly from locations of its unsecured or inappropriate storage, areas of animal husbandry, and where deposits of the substance are undergoing removal (Larsbo et al., 2016). Chlorfenvinphos can penetrate into the atmosphere following its use in agriculture as an aerosol sprayed by ground application. In this manner, only a part of the compound reaches its target directly. Only 1% of the sprayed pesticide is delivered into the intended target (Kumar et al., 2015). The remaining part is released in an unintended manner and enters the surface and ground water as well as the atmosphere (Akyil et al., 2016). Toxicity tests in reaction mixtures before and after advanced oxidation processes were conducted using the bacteria *Aliivibrio fischeri* (MICROTOX® biotest) and the dicotyledon embryophyte Lepidium sativum (phytotoxicity tests). The bioluminescence inhibition of the bacteria *Aliivibrio fischeri* was measured using the Microtox 500 analyser (Tigret Sp. z o.o., Warsaw, Poland) after 5 and 15 min of exposure and then compared to the control sample (2% NaCl). No significant differences were found between the 5 and 15 min times, therefore an exposure time of 5 minutes was selected for the data analysis. The aqueous solution toxicity was determined based on a toxicity classification system in accordance with known guidelines (Dudziak 2017). The toxicity classification is presented in Table 1.

The phytotoxicity testing on Lepidium sativum was conducted in accordance with ISO 11269-2 (ISO 11269:2-2012 2012) and the OECD guidelines (OECD 2006). Before commencing the toxicological testing, the germination rate of seeds left in the dark at a temperature of 21 °C was inspected. Seeds with a germination rate exceeding 90% were selected for further testing. The phytotoxicity test was carried out on 20 seeds laid out on Petri dishes covered with filter paper. The tests were conducted in a dark space, at ambient temperature (25 °C), for 72 hours. Control tests were performed parallel to the main tests. The

Table 1. Toxicity classification system for aqueous solutions (Dudziak 2017)

Inhibition of bioluminescence [%]	Toxicity classification
< 25	Non-toxic
25–50	Low toxicity
50.1–75	Toxic
75.1–100	High toxicity

inhibition or stimulation was determined based on the stem and root growth measured relative to the control samples. The test was performed twice for each of the reaction mixtures. Based on the number of germinating seeds in a sample and the control sample as well as the average plant root growth in the main test and the control test, germination index (GI) calculations were performed with reference to the roots per formula (2) (Czop et al., 2016).

$$GI = \frac{(G_S \cdot R_T)}{(G_T \cdot R_C)} \cdot 100 \quad (2)$$

where: *GI* – germination index [%], *GS* – number of germinated seeds [-], *RT* – average length of plant roots in the test sample [mm], *GT* – number of total seeds [-], *RC* – average length of plant roots in the control sample [mm].

RESULTS AND DISCUSSION

Advanced oxidation experiments

Ozonation

Organic compound degradation in the presence of ozone occurs following a direct or indirect mechanism. Both the reactions occur simultaneously, therefore it is difficult to separate them and determine the specific degradation mechanisms. Generally, low pH (< 4) facilitates direct pollutant oxidation by ozone. On the other hand, higher pH is conducive to indirect oxidation by •OH (Beltrán and Rey, 2018). The lower the pH, the lower the hydroxyl radical generation rate. Reactions with •OH are dominant at higher pH, therefore this test maintained a pH close to neutral (pH = 6.0).

The O_3 dose has a significant influence on CFVP degradation. Figure 1 demonstrates that after 45 minutes the CFVP removal was set to 44−62%. The higher the ozone dose, the shorter the time required for the CFVP degradation. The increase of the dose in the reaction system leads to an increased likelihood of CFVP molecule collisions with the rising concentrations of O_3 and the •OH radical (Han et al., 2022). Reactions of pollutant molecules with •OH radicals occur primarily by the removal of H from C-H, N-H or O-H bonds or its addition to C=C bonds. The greatest removal level was achieved at an ozone dose of 125 mg/L, though 100 mg/L was selected as the economically feasible dose. The differences between these doses were insignificant. On the one hand, increasing the ozone dose also increases the degradation efficiency, but on the other it carries the potential risk of increased oxidation by-product generation (Pulicharla et al., 2020).

Influence of UV light in O_3 process

Figure 2 demonstrates that after 45 minutes the CFVP removal was set to 62−80%. The greatest removal level was obtained at an ozone dose of 125 mg/L, though the differences between the 100 mg/L and 125 mg/L doses were negligible. CFVP degradation is a result of numerous

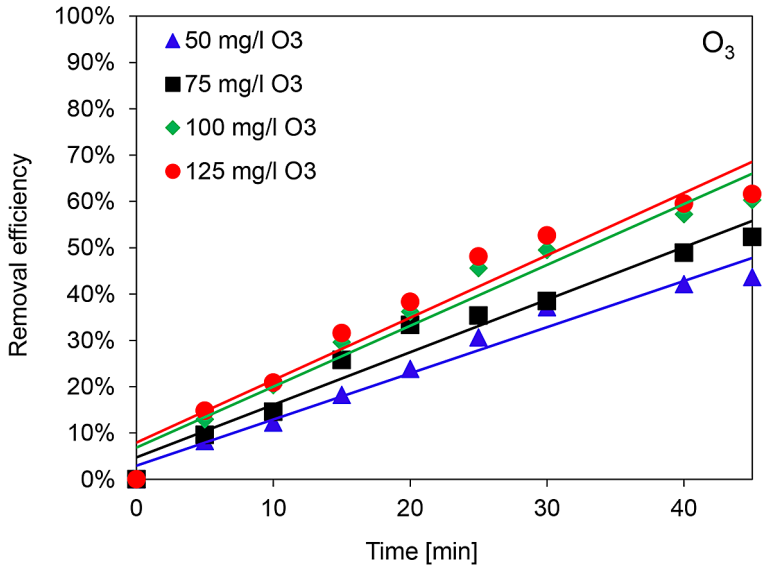

Figure 1. Effect of initial ozone dose on CVFP removal in O_3 process ($C_{0[CFVP]}$ = 50 µg/L; V = 0.4 L; T = 295.0 K; pH = 6.0; t = 0– 45 min)

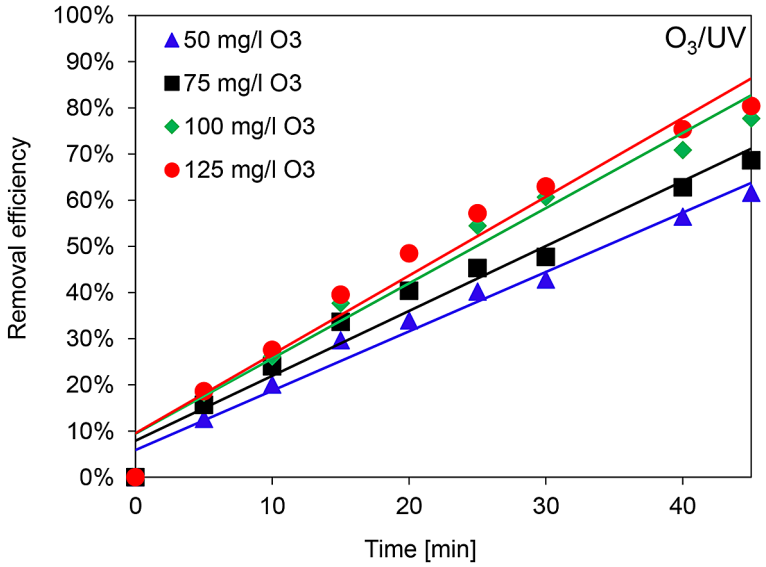

Figure 2. Effect of initial O_3 dose on CVFP removal in O_3/UV process ($C_{0[CFVP]}$ = 50 µg/L; V = 0.4 L; T = 295.0 K; pH = 6.0; t = 0– 45 min)

reactions, but in the case of AOPs the two-stage model is the most frequently cited one (Cuerda-Correa et al., 2020). It consists primarily in the photoinduced homolysis of ozone molecules followed by hydroxyl radical generation through a reaction of water with atomic oxygen. The •OH radical generation mechanism in the O_3/UV process is presented in formulas (3–5) (Sofia 2020).

$$O_3 \rightarrow O_2 + O \quad (3)$$

$$O_3 + O \rightarrow 2O_2 \quad (4)$$

$$O + H_2O \rightarrow 2OH\bullet \quad (5)$$

The combined ultraviolet-assisted ozonation process (O_3/UV) generates more •OH radicals, while the reaction itself occurs at a broader range of pH (Sgroi et al. 2021). Yang et al. (2024) indicated an optimal reaction value of pH = 6.7. Combining ozonation and UV yields an efficient method of pollutant degradation (Jabbari et al., 2020).

Effect of TiO_2 dosage

In the photocatalytic process conducted in the presence of TiO_2 it is necessary to provide radiation with the appropriate wavelength, carrying energy higher than the band gap energy. The minimum energy required for activation equals the band gap energy and amounts to Eg = 3.02 V for TiO_2 in the form of rutile and Eg = 3.20 V for TiO_2 in the form of anatase (Armaković et al., 2023). TiO_2 can be activated by the energy of light with a wavelength λ = 400 nm, therefore it is necessary to supply lamps that emit ultraviolet radiation within λ = 300–388 nm (Al-Nuaim et al., 2023). Semiconductor excitation results in electron transfer from the valence band (VB) to the conduction band (CB). An electron hole is formed, which corresponds to the generation of redox potential on the photocatalyst molecule surface (Macedo et al., 2022). The photocatalyst is activated by the effects of the UV radiation, while numerous reactions lead to the formation of electron holes that react with water molecules, resulting in •OH radical generation.

At a dose of 50 mg/L, the CFVP removal level after 20 min of reaction time was set to 20%. Extending the reaction time to 45 min resulted in an increase of the efficiency to 42% (Figure 3). Garg et al. (2019) conducted bisphenol A degradation at doses ranging within 20–175 mg/L. On the other hand, refinery wastewater tests utilised a dose of even 700 mg/L (Aljuboury and Shaik, 2021). Therefore, the TiO_2 dose was doubled (100 mg/L), and consequently the CFVP degradation was set to 34% after 20 min, and 56% after 45 min. A dose of 75 mg/L was adopted as optimal given the negligible differences in the CFVP removal. Generally, the photocatalyst dose applied for the CFVP degradation was not significantly different from doses used in the removal of other organophosphorus pesticides. For example, the study by Sharma et al. (2016) used a catalyst dose of 160 mg/L for the degradation of parathion methyl and parathion. Mirmasoomi et al. (2017)

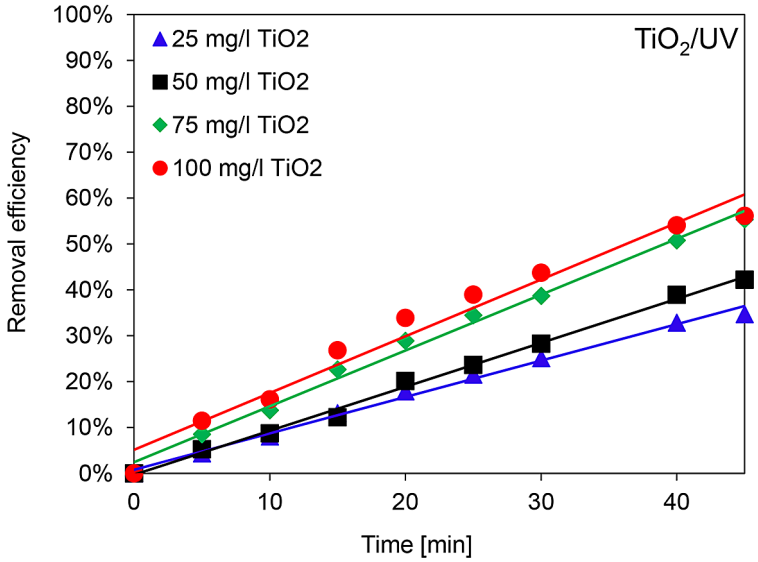

Figure 3. Effect of initial TiO_2 dose on CVFP removal in TiO_2/UV process ($C_{0[CFVP]}$ = 50 µg/L; V = 0.4 L; T = 295.0 K; pH = 6.0; t = 0– 45 min)

applied a dose of 100 mg/L for diazinon degradation. It should be noted that the application of higher photocatalyst doses can lead to negative phenomena resulting in reduced degradation efficiency. For example, these include TiO_2 molecule agglomeration or rapid photocatalyst molecule sedimentation. Esmaili et al. (2018) demonstrated that increasing the catalyst dose can reduce light penetration in a solution in the heterogeneous photooxidation process. This therefore substantiates a reduction in the TiO_2 dosage.

Effect of different PS concentration in PS/Vis

The CFVP degradation was conducted by means of sulfate radicals ($SO_4^{\bullet-}$). SPS activation results from the synergistic interaction of visible light and glucose. Exposing the solutions to visible light leads to glucose decomposition, electron transfer from the sugar towards the SPS (SPS activation) and the oxidation of glucose into SPS-activating products (Cai et al., 2019). The PS dose has a significant influence on CFVP removal. Figure 4 demonstrates

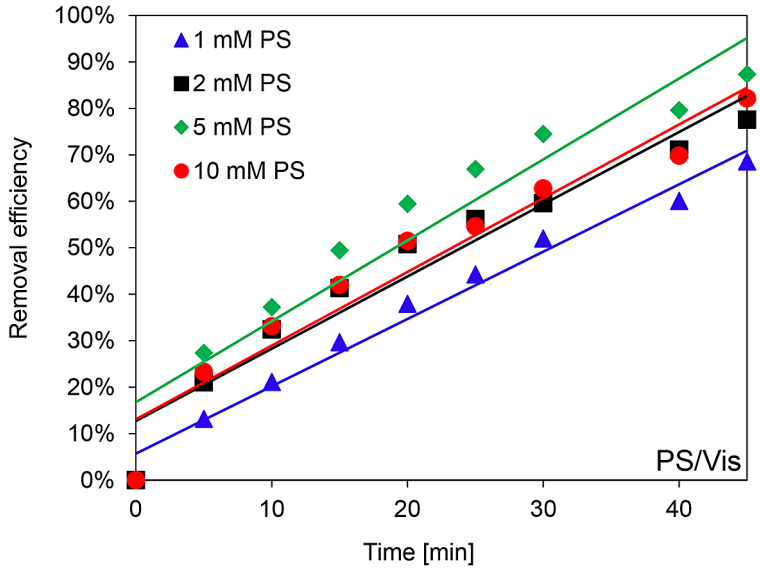

Figure 4. Effect of initial PS dose on CVFP removal in PS/Vis process (C0[CFVP] = 1.0 mg/L; V = 0.4 L; T = 295.0 K; pH = 6.0; t = 0– 45 min)

that after 45 minutes the CFVP removal was set to 69−87%. The greatest removal level was obtained at a SPS dose of 5 mM (45 min). Applying a higher dose leads to a lower CFVP removal level due to the molecule aggregation or oxidation of the sulfate radicals by other oxidative compounds, e.g. $S_2O_8^{2-}$ (Lv et al. 2022). This phenomenon is characteristic of various processes, with the participation of both $SO_4^{\bullet-}$ and •OH radicals. In the study by Rizal et al. (2021), a SPS concentration of over 30 mM resulted in lower methylene blue decolourisation efficiency. As concluded by Saien and Jafari (2022), a higher SPS dose leads to a lower treatment efficiency due to a reaction between the sulfate anion and hydroxyl radicals.

Influence of CFVP concentration

The influence of the initial CFVP concentration ($C_{0[CFVP]}$) was determined for O_3, O_3/UV, TiO_2/UV and PS/Vis processes using optimal parameters adopted in prior experiments. Figure 5 reveals that after 30 minutes the CFVP removal was set to 12%−92%, depending on the $C_{0[CFVP]}$ and the process itself. An increase in $C_{0[CFVP]}$ disturbs processes involving oxidative radicals. Regardless of the process, the phenomenon of decreased degradation efficiency occurs together with the increasing CFVP concentration. This phenomenon is typical of nearly all oxidation processes (Kocijan et al., 2022), including advanced oxidation processes (John et al., 2020). It is a consequence of the increasing pollutant molecule concentration and the lower likelihood of oxidative radical collision with the pollutant molecules (Mortazavian et al., 2019). For example, Hanafi and Sapawe (2020) observed a reduction in the Remazol Brilliant Blue dye degradation efficiency in the NiO/UV process from 90% to 36% after a tenfold increase of the dye concentration. In AOPs involving light, the most likely reason for this is that the light cannot penetrate into solutions at high concentration, which ultimately leads to a lower oxidative radical production (Muthukumar et al., 2021). As regards processes using persulfates, Liu et al. (2018) and Han et al. (2020) also noted a similar phenomenon.

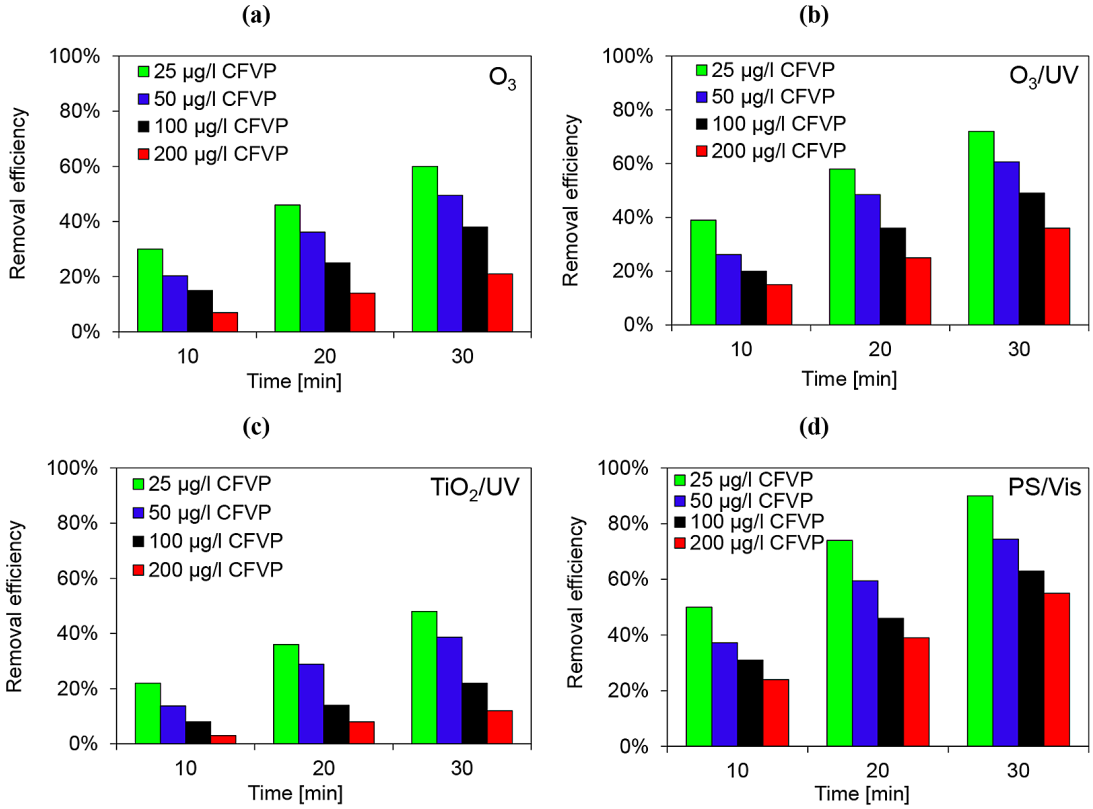

Figure 5. Effect of initial CFVP concentration on CVFP removal in (a) O_3, (b) O_3/UV, (c) TiO_2/UV and (d) PS/Vis processes (ozone dose = 100 mg/L; TiO_2 dose = 75 mg/L; SPS dose = 5 mM; V = 0.4 L; T = 295.0 K; pH = 6.0; t = 10– 30 min)

TOC removal

A high removal efficiency does not always correspond to total pollutant mineralisation. Oxidation processes are often accompanied by oxidation by-product generation. Oxidation by-products can be characterised by a toxicity greater than the originally removed compounds (Rayaroth et al., 2022). Determining the remaining total organic carbon (TOC) content can therefore be the basis for the further enhancement of the processes. Figure 6 presents the effects of %TOC removal over a time of 30 minutes. The highest %TOC removal effects are provided by the PS/Vis process. This is a result of the higher oxidation potential of the $SO_4^{\bullet-}$ radical compared to •OH as well as the longer half-life of the $SO_4^{\bullet-}$ radical. The oxidation potential of •OH is 1.8 V–2.80 V, whereas for the $SO_4^{\bullet-}$ radical it is 2.5 V–3.1 V, and the half-life of •OH is < 1 µs, which for $SO_4^{\bullet-}$ is 30–40 µs (Li et al., 2019; Xia et al., 2020). The obtained results proved better relative to those obtained by Aimer et al. (2019), where the degradation of dimethoate involved electrolysis and oxidation by sulfate radicals generated by thermal methods. About 40% of %TOC removal over a time of 120 min was obtained by electrolysis compared to just 10% by oxidation involving sulfate radicals generated by thermal methods. On the other hand, the studies by Žabar et al. (2016) yielded about 54% of TCP (3,5,6-trichloro-2-pyridinol) mineralisation efficiency after 120 minutes of photodegradation by TiO_2/UVA.

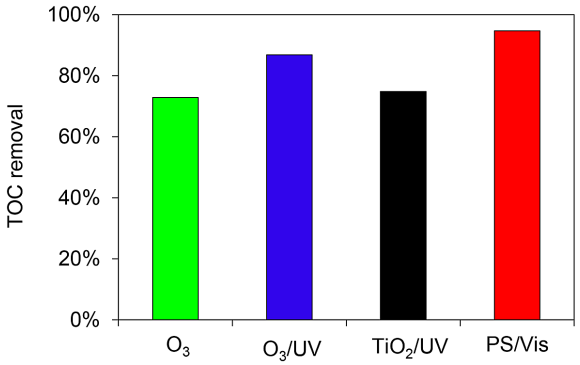

Figure 6. TOC removal during different AOPs ($C_{0[CFVP]}$ = 50 µg/L; ozone dose = 100 mg/L; TiO_2 dose = 75 mg/L; SPS dose = 5 mM; V = 0.4 L; T = 295.0 K; pH = 6.0; t = 30 min)

Evaluation of toxicity

The tools applied to control the post-process solution quality included biological tests with bacteria (*Aliivibrio fischeri*) and plants (*Lepidium sativum*). The choice was motivated by the different sensitivity of the organisms to external conditions. Generally, *Aliivibrio fischeri* are more sensitive than *Lepidium sativum* (Tongur and Yıldız, 2021). The primary advantages of biological tests with Lepidium sativum include the availability of various methods of toxicity assessment, e.g. root and stem growth measurement as well as cost efficiency (Rueda-Márquez et al., 2020). On the other hand, tests with *Aliivibrio fischeri* are characterised by sensitive reactions and low costs, and are also environmentally friendly (Zhang et al., 2023).

Toxicity tests with Aliivibrio fischeri

As shown in Figure 7, both the TiO_2/UV and PS/Vis processes result in a reduction of toxicity to safe levels (low toxicity). However, only by PS/Vis is it possible to obtain a sample characterised by no toxicity (< 20% relative to

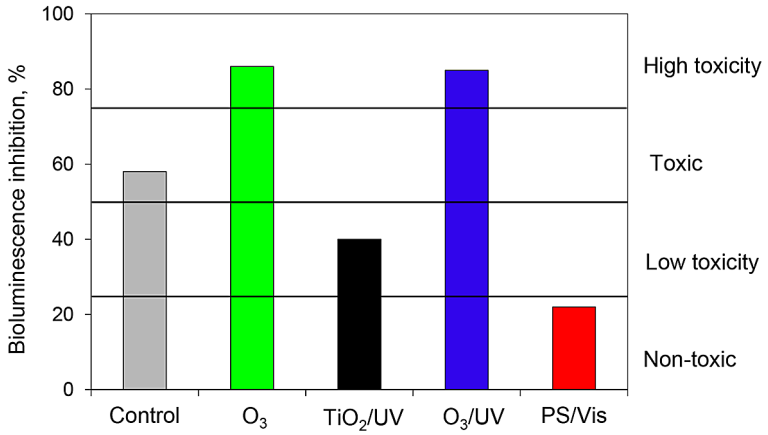

Figure 7. Inhibition of bioluminescence during different AOPs ($C_{0[CFVP]}$ = 50 µg/L; ozone dose = 100 mg/L; TiO_2 dose = 75 mg/L; SPS dose = 5 mM; V = 0.4 L; T = 295.0 K; pH = 6.0; t = 30 min)

the *Aliivibrio fischeri* bacteria). As suggested by Miralles-Cuevas et al. (2017), an inhibition higher than 30% is still considered toxic. As also presented, in AOPs involving ozone, the sample toxicity increases and is higher compared to the control sample containing only CFVP. Ozone is one of the strongest oxidisers, and it is applied for water disinfection (Gorito et al., 2021). This is the likely reason for the negative biological effect of the sample. Furthermore, ozonation generates a broad range of carbonyl disinfection by-products, including carboxylic acids, aldehydes, ketones and aldo-keto acids. In the case of CFVP degradation, these can include toxic aromatic acids or esters, as well as toxic 2,4-dichlorobenzoic acid or triethyl phosphate.

Toxicity tests with Lepidium sativum

The post-process solution toxicity was also evaluated by means of *Lepidium sativum*. The results were compared to a control sample (deionised water) and a sample synthetically polluted with CFVP (50 µg/L) (Figure 8). Comparably to the toxicity results with *Aliivibrio fischeri*, ozonation and O_3/UV resulted in the highest toxicity towards plants, as could be deduced from the low %GI (Figure 9). The photocatalytic reaction yielded a higher %GI than O_3 and O_3/UV (56%). However, only the PS/Vis process was capable of reducing the phytotoxicity of the initial solution to a non-toxic level (GI = 79%). The performed tests confirm that in the case of a higher %TOC residue, the toxic effect of the sample is retained even after 30 minutes of AOP conduction. The *Lepidium sativum* seeds exhibited higher germination indices (GI) after exposure to the effects of the post-process solutions relative to the toxicity towards *Aliivibrio fischeri*, which could be related to the various generated by-products (Fernandes et al., 2020).

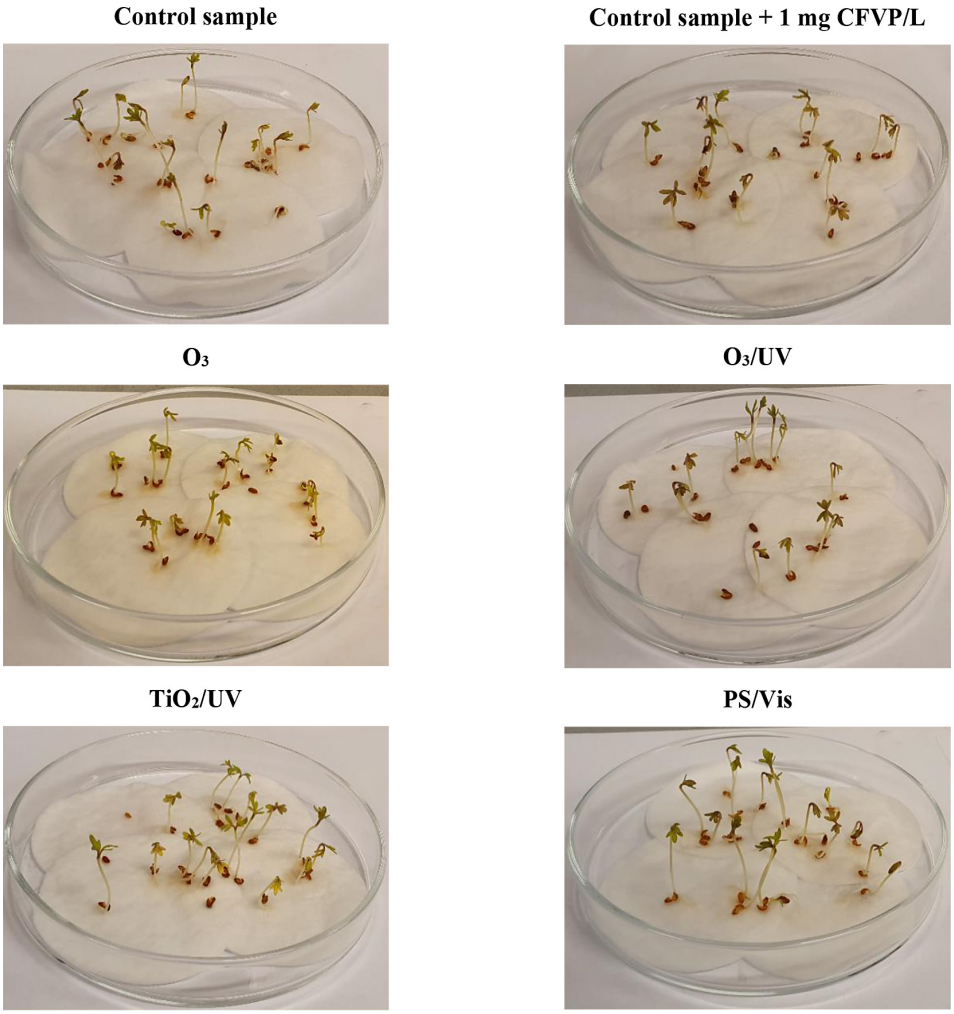

Figure 8. Growth of Lepidium sativum during different AOPs ($C_{0[CFVP]}$ = 50 µg/L; ozone dose = 100 mg/L; TiO_2 dose = 75 mg/L; SPS dose = 5 mM; V = 0.4 L; T = 295.0 K; pH = 6.0; t = 30 min)

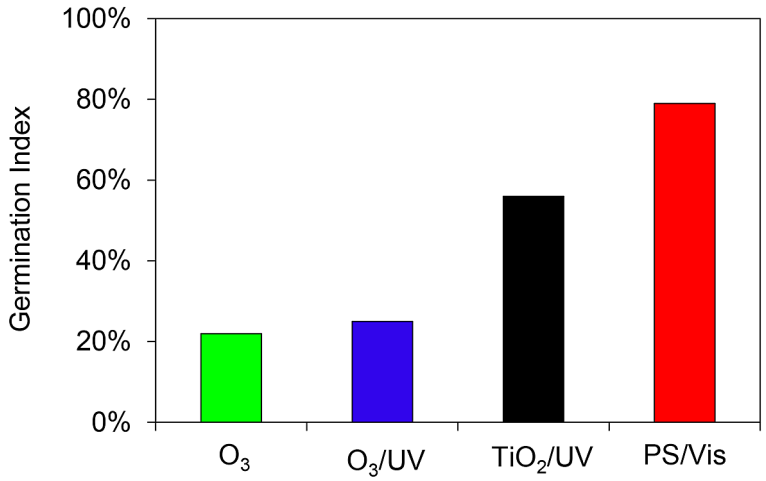

Figure 9. Germination Index of Lepidium sativum during different AOPs ($C_{0[CFVP]}$ = 50 µg/L; ozone dose = 100 mg/L; TiO_2 dose = 75 mg/L; SPS dose = 5 mM; V = 0.4 L; T = 295.0 K;

Comparison with other pesticides removal technologies

Table 2 shows that the proposed method is an interesting alternative for CFVP elimination compared to previous studies performed by other researchers. As evidenced, the PS/Vis process has a high potential for CFVP degradation, especially where the dye concentration is not very high (up to about 100 µg/L). This shows the benefit of the PS/Vis process, which targets wastewater treatment as the next purification step. Energy-efficient equipment, relatively short reaction time (30.0 min) and low reagent consumption are advantages of this method. After 30 min in PS/Vis, CFVP degradation was found to be 90%. This time was shorter than in (Lapertot et al., 2006; Oliveira et al., 2014), where 94–97% of the pesticide was removed after 50–60 min of reaction. The proposed method is characterized by low power of the radiation source (10 W compared to 500 W in the study (Roselló-Márquez et al., 2021) and 1000 W in the study (Fernández-Domene et al., 2019). The advantage of the process studied is a pH close to neutral (pH = 6.0), which is important from an environmental and operating cost perspective. Compared to other processes, such as the Fenton process (Oliveira et al., 2014), a low pH (pH = 3.0) is not required, which is in favor of the PS/Vis process.

CONCLUSIONS

This study compared four advanced chlorfenvinphos oxidation processes: O_3, O_3/UV, TiO_2/UV and PS/Vis. In order to obtain samples with the lowest possible toxicity, a selection of the basic process parameters determining the environmentally safe treatment of chlorfenvinphos-polluted solutions was performed (O_3 dose, TiO_2 dose and SPS dose). Based on the conducted tests, it was demonstrated that the PS/Vis process is characterised by the highest CFVP degradation efficiency. As a result, CFVP reduction at a level of 55–90% was achieved at a concentration of 5 µg/L to 200 µg/L under the following conditions: SPS dose = 5 mM; V = 0.4 L; T = 295.0 K; pH = 6.0; t = 30 min. Even in the case of optimal process conditions, each of the processes exhibited a residue of TOC, which may suggest the generation of oxidation by-products. Identifying the residual TOC may be the basis for the further enhancement of AOPs. The post-process solution toxicity was analysed using *Lepidium sativum* (garden cress) and the bacteria *Aliivibrio fischeri*. The TiO_2/UV and PS/Vis processes provide a reduction of toxicity to safe levels (low toxicity). Only the PS/Vis process yields an environmentally safe sample characterised by a bioluminescence inhibition < 20% relative to the *Aliivibrio fischeri* bacteria. Similar results were obtained for *Lepidium sativum*. The divergent toxicity results relative to various organisms can be related to different generated by-products. This substantiates the necessity to conduct toxicity tests on various organisms with different sensitivity. The experimental testing demonstrated that optimal process conditions result in the highest efficiency of CFVP degradation and improved biological safety. It was found that the PS/Vis process can be a valuable alternative to O_3, O_3/UV and TiO_2/UV.

Table 2. Efficiency of Chlorfenvinphos degradation in removal technologies

Pesticide	Process	Conditions	Efficiency [%]	Literature
Chlorfenvinphos	PS/Vis	Run time = 30 min; SPS dose = 5 mM; V = 0.4 L; T = 295.0 K; C_0 = 25 µg/L; pH = 6.0 Type of lamp = tungsten Lamp power = 10 W	90	This study
Chlorfenvinphos	Fenton	Run time = 60 min $[H_2O_2]:[Fe^{2+}]$ = 32.6 T = 303.15 K C_0 = 100 mg/L pH = 3.0	97	(Oliveira et al. 2014)
Chlorfenvinphos	Biodegradation in medicinal plants	Run time = 30 min Vegetation = Calendula Officinalis and Tagetes Patula C_0 = 100 µg/L Amount of flower samples = 0.5–1 g	26 (Calendula Officinalis) 33 (Tagetes Patula)	(Puiu et al. 2017)
Chlorfenvinphos	Visible-light driven photoelectrochemical degradation in the presence of WO_3 nanosheets / nanorods	Thermal treatment (annealing) of nanostructured electrodes = 873.15 K Run time = 360 min pH = 1 C_0 = 20 mg/l T = 293.15 K The bias potential (vs. SCE) = +1 V Type of lamp = Xe lamp Lamp power = 1000 W	95	(Fernández-Domene et al. 2019)
Chlorfenvinphos	Photodegradation by using WO_3 nanostructures	Thermal treatment (annealing) of nanostructured electrodes = 873.15 K Anodization in electrolyte: 1.5 M CH_4O_3S; 0.05 M H_2O_2 Run time = 1 440 min The bias potential (vs. SCE) = +1 V C_0 = N/D T = room temperature Type of lamp = Xe lamp Lamp power = 500 W	95	(Roselló-Márquez et al. 2021)
Chlorfenvinphos	Photo-Fenton	pH = 2.7 – 2.8 Run time = 50 min H_2O_2 = 400 mg/L Fe^{2+} = 20 mg/L C_0 = 50 mg/L $[H_2O_2]:[Fe^{2+}]$ = 20 Lamp = 30 W/m^2	94	(Lapertot et al. 2006)
Chlorfenvinphos	Gamma-irradiation	γ-irradiation a ^{60}Co = 3 kGy C_0 = 5.0 µg/mL pH = 6.2	60–81	(Khedr et al. 2019)

Acknowledgements

The presented study was performed in the framework of the research work in the Central Mining Institute – National Research Institute in Poland, financially supported by the Polish Ministry of Science and Higher Education [No. 11131013-340].

REFERENCES

1. 2013/39/EU (2013) Directive 2013/39/EU of the European Parliament and of the Council of 12 August 2013 amending Directives 2000/60/EC and 2008/105/EC as regards priority substances in the field of water policyText with EEA relevance.
2. Abbas M, Adil M, Ehtisham-ul-Haque S, et al (2018) Vibrio fischeri bioluminescence inhibition assay for ecotoxicity assessment: A review. *Science of The Total Environment 626*:1295–1309. https://doi.org/10.1016/j.scitotenv.2018.01.066
3. Ahmadi S, Osagie C, Rahdar S, et al (2020) Efficacy of persulfate-based advanced oxidation process (US/PS/Fe_3O_4) for ciprofloxacin removal from aqueous solutions. *Appl Water Sci 10*:187. https://doi.org/10.1007/s13201-020-01271-7
4. Aimer Y, Benali O, Groenen Serrano K (2019) Study of the degradation of an organophosphorus pesticide using electrogenerated hydroxyl radicals or heat-activated persulfate. *Separation and Purification Technology 208*:27–33. https://doi.org/10.1016/j.seppur.2018.05.066
5. Akyil D, Ozkara A, Konuk M (2016) *Pesticides, Environmental Pollution, and Health.* Chapters
6. Alderete BL, da Silva J, Godoi R, et al (2021) Evaluation of toxicity and mutagenicity of a synthetic effluent containing azo dye after Advanced Oxidation Process treatment. *Chemosphere 263*:128291. https://doi.org/10.1016/j.chemosphere.2020.128291
7. Aljuboury D al deen A, Shaik F (2021) Assessment of TiO_2/ZnO/H_2O_2 Photocatalyst to treat wastewater from oil refinery within visible light circumstances. *South African Journal of Chemical Engineering 35*:69–77. https://doi.org/10.1016/j.sajce.2020.11.004
8. Al-Nuaim MA, Alwasiti AA, Shnain ZY (2023) The photocatalytic process in the treatment of polluted water. *Chem Pap 77*:677–701. https://doi.org/10.1007/s11696-022-02468-7
9. Ameta SC (2018) *Introduction. In: Advanced Oxidation Processes for Waste Water Treatment.* Elsevier, 1–12.
10. Armaković SJ, Savanović MM, Armaković S (2023) titanium dioxide as the most used photocatalyst for water purification: An overview. *Catalysts 13*:26. https://doi.org/10.3390/catal13010026
11. Barbieri MV, Peris A, Postigo C, et al (2021) Evaluation of the occurrence and fate of pesticides in a typical Mediterranean delta ecosystem (Ebro River Delta) and risk assessment for aquatic organisms. *Environmental Pollution 274*:115813. https://doi.org/10.1016/j.envpol.2020.115813
12. Beltrán FJ, Rey A (2018) free radical and direct ozone reaction competition to remove priority and pharmaceutical water contaminants with single and hydrogen peroxide ozonation systems. *Ozone: Science & Engineering 40*:251–265. https://doi.org/10.1080/01919512.2018.1431521
13. Cabascango T, Ortiz K, Sandoval Pauker C, et al (2021) Assessment of advanced oxidation processes using zebrafish in a non-forced exposure system: a proof of concept. *Processes 9*:734. https://doi.org/10.3390/pr9050734
14. Cai T, Liu Y, Wang L, et al (2019) Activation of persulfate by photoexcited dye for antibiotic degradation: Radical and nonradical reactions. *Chemical Engineering Journal 375*:122070. https://doi.org/10.1016/j.cej.2019.122070
15. Cerejeira MJ, Viana P, Batista S, et al (2003) Pesticides in Portuguese surface and ground waters. *Water Research 37*:1055–1063. https://doi.org/10.1016/S0043-1354(01)00462-6
16. Chief Inspectorate for Environmental Protection (2016) State Environmental Monitoring, surface water research results – rivers.
17. Cuerda-Correa EM, Alexandre-Franco MF, Fernández-González C (2020) Advanced oxidation processes for the removal of antibiotics from water. An Overview. *Water 12*:102. https://doi.org/10.3390/w12010102
18. Czop M, Czoch D, Korol A, Maduzia A (2016) Tests of phytotoxicity of ashes from low-rise buildings on selected group of plants. *Archiwum Gospodarki Odpadami i Ochrony Środowiska 18*.
19. Delardas O, Giannos P (2022) The ripple effects of the energy crisis on academia. *EMBO reports 23*:e56287. https://doi.org/10.15252/embr.202256287
20. Dong G, Chen B, Liu B, et al (2022) Comparison of O3, UV/O3, and UV/O3/PS processes for marine oily wastewater treatment: Degradation performance, toxicity evaluation, and flocs analysis. *Water Res 226*:119234. https://doi.org/10.1016/j.watres.2022.119234
21. Dudziak M (2017) Influence of the aquatic environment conditions on the decomposition of bisphenol A. *Ecological Chemistry and Engineering A 24*. https://doi.org/10.2428/ecea.2017.24(2)14
22. Environment Agency (1997) The occurrence of sheep-dip pesticides in environmental waters

23. Esmaili H, Kotobi A, Sheibani S, Rashchi F (2018) Photocatalytic degradation of methylene blue by nanostructured Fe/FeS powder under visible light. *Int J Miner Metall Mater 25*:244–252. https://doi.org/10.1007/s12613-018-1567-x
24. Fernandes E, Contreras S, Medina F, et al (2020) N-doped titanium dioxide for mixture of parabens degradation based on ozone action and toxicity evaluation: Precursor of nitrogen and titanium effect. *Process Safety and Environmental Protection 138*:80–89. https://doi.org/10.1016/j.psep.2020.03.006
25. Fernández-Domene RM, Roselló-Márquez G, Sánchez-Tovar R, et al (2019) Photoelectrochemical removal of chlorfenvinphos by using WO3 nanorods: Influence of annealing temperature and operation pH. *Separation and Purification Technology 212*:458–464. https://doi.org/10.1016/j.seppur.2018.11.049
26. Foka Wembe EN, Benghafour A, Dewez D, Azzouz A (2023) Clay-catalyzed ozonation of organic pollutants in water and toxicity on lemna minor: effects of molecular structure and interactions. *Molecules 28*:222. https://doi.org/10.3390/molecules28010222
27. Foszpańczyk M, Drozdek E, Gmurek M, Ledakowicz S (2018) Toxicity of aqueous mixture of phenol and chlorophenols upon photosensitized oxidation initiated by sunlight or vis-lamp. *Environ Sci Pollut Res Int 25*:34968–34975. https://doi.org/10.1007/s11356-018-1286-x
28. Garg A, Singhania T, Singh A, et al (2019) Photocatalytic degradation of bisphenol-A using N, Co codoped TiO_2 catalyst under solar light. *Scientific Reports 9*:1–13. https://doi.org/10.1038/s41598-018-38358-w
29. Gorito AM, Pesqueira JFJR, Moreira NFF, et al (2021) Ozone-based water treatment (O3, O3/UV, O3/H2O2) for removal of organic micropollutants, bacteria inactivation and regrowth prevention. *Journal of Environmental Chemical Engineering 9*:105315. https://doi.org/10.1016/j.jece.2021.105315
30. Han F, Ye X, Chen Q, et al (2020) The oxidative degradation of diclofenac using the activation of peroxymonosulfate by $BiFeO_3$ microspheres—Kinetics, role of visible light and decay pathways. *Separation and Purification Technology 232*:115967. https://doi.org/10.1016/j.seppur.2019.115967
31. Han Q, Dong W, Wang H, et al. (2022) Performance of ozonation on bisphenol a degradation: Efficiency, mechanism and toxicity control. *Frontiers in Environmental Science 10*.
32. Hanafi MF, Sapawe N (2020) Effect of initial concentration on the photocatalytic degradation of remazol brilliant blue dye using nickel catalyst. *Materials Today: Proceedings 31*:318–320. https://doi.org/10.1016/j.matpr.2020.06.066
33. Honarmandrad Z, Sun X, Wang Z, et al (2023) Activated persulfate and peroxymonosulfate based advanced oxidation processes (AOPs) for antibiotics degradation – A review. *Water Resources and Industry 29*:100194. https://doi.org/10.1016/j.wri.2022.100194
34. ISO 11269:2-2012 (2012) ISO 11269-2:2012 - Soil quality - Determination of the effects of pollutants on soil flora - Part 2: Effects of contaminated soil on the emergence and early growth of higher plants. In: ISO. https://www.iso.org/standard/51382.html. Accessed 13 Aug 2024
35. ISO 11369 (1997) EN 11369 - Water quality - Determination of selected plant treatment agents - Method using high performance liquid chromatography with UV detection after solid-liquid extraction. In: ISO. https://www.iso.org/standard/19314.html. Accessed 13 Aug 2024
36. Jabbari F, Eslami A, Mahmoudian J (2020) Degradation of diclofenac in water using the O_3/UV/S_2O_8 advanced oxidation process. *Health Scope 9*. https://doi.org/10.5812/jhealthscope.99436
37. John D, Rajalakshmi AS, Lopez RM, Achari VS (2020) TiO2-reduced graphene oxide nanocomposites for the trace removal of diclofenac. *SN Appl Sci 2*:840. https://doi.org/10.1007/s42452-020-2662-y
38. Khedr T, Hammad AA, Elmarsafy AM, et al (2019) Degradation of some organophosphorus pesticides in aqueous solution by gamma irradiation. *Journal of Hazardous Materials 373*:23–28. https://doi.org/10.1016/j.jhazmat.2019.03.011
39. Kocijan M, Ćurković L, Gonçalves G, Podlogar M (2022) The potential of rGO@TiO_2 photocatalyst for the degradation of organic pollutants in water. *Sustainability 14*:12703. https://doi.org/10.3390/su141912703
40. Koranteng SS, Darko DA, Nukpezah D, Ameka GK (2018) Pesticides bioconcentration potential of aquatic plants in the Volta Lake. *West African Journal of Applied Ecology 26*:193–202. https://doi.org/10.4314/wajae.v26i0
41. Kowalska E, Janczarek M, Hupka J, Grynkiewicz M (2004) H_2O_2/UV enhanced degradation of pesticides in wastewater. *Water Science and Technology 49*:261–266. https://doi.org/10.2166/wst.2004.0279
42. Kumar P, Kim K-H, Deep A (2015) Recent advancements in sensing techniques based on functional materials for organophosphate pesticides. *Biosensors and Bioelectronics 70*:469–481. https://doi.org/10.1016/j.bios.2015.03.066
43. Lambropoulou D, Evgenidou E, Saliverou V, et al (2017) Degradation of venlafaxine using TiO_2/UV process: Kinetic studies, RSM optimization, identification of transformation products and

toxicity evaluation. *Journal of Hazardous Materials 323*:513–526. https://doi.org/10.1016/j.jhazmat.2016.04.074

44. Lapertot M, Pulgarín C, Fernández-Ibáñez P, et al (2006) Enhancing biodegradability of priority substances (pesticides) by solar photo-Fenton. *Water Research 40*:1086–1094. https://doi.org/10.1016/j.watres.2006.01.002
45. Larsbo M, Sandin M, Jarvis N, et al (2016) Surface Runoff of Pesticides from a Clay Loam Field in Sweden. *Journal of Environmental Quality 45*:1367–1374. https://doi.org/10.2134/jeq2015.10.0528
46. Lellis B, Fávaro-Polonio CZ, Pamphile JA, Polonio JC (2019) Effects of textile dyes on health and the environment and bioremediation potential of living organisms. *Biotechnology Research and Innovation 3*:275–290. https://doi.org/10.1016/j.biori.2019.09.001
47. Li J, Li Y, Xiong Z, et al (2019) The electrochemical advanced oxidation processes coupling of oxidants for organic pollutants degradation: A mini-review. *Chinese Chemical Letters 30*:2139–2146. https://doi.org/10.1016/j.cclet.2019.04.057
48. Liu F, Yi P, Wang X, et al (2018) Degradation of Acid Orange 7 by an ultrasound/ZnO-GAC/persulfate process. *Separation and Purification Technology 194*:181–187. https://doi.org/10.1016/j.seppur.2017.10.072
49. Lv X, Leng Y, Wang R, et al (2022) Persulfate activation by ferrocene-based metal–organic framework microspheres for efficient oxidation of orange acid 7. *Environ Sci Pollut Res.* https://doi.org/10.1007/s11356-022-18669-2
50. Macedo OB de, Oliveira ALM de, Santos IMG dos (2022) Zinc tungstate: a review on its application as heterogeneous photocatalyst. *Cerâmica 68*:294–315. https://doi.org/10.1590/0366-69132022683873265
51. Mahmoudi S, Fadaei S, Taheri E, et al (2022) Direct red 89 dye degradation by advanced oxidation process using sulfite and zero valent under ultraviolet irradiation: Toxicity assessment and adaptive neuro-fuzzy inference systems modeling. *Environmental Research 211*:113059. https://doi.org/10.1016/j.envres.2022.113059
52. Miralles-Cuevas S, Oller I, Agüera A, et al (2017) Strategies for reducing cost by using solar photo-Fenton treatment combined with nanofiltration to remove microcontaminants in real municipal effluents: Toxicity and economic assessment. *Chemical Engineering Journal 318*:161–170. https://doi.org/10.1016/j.cej.2016.06.031
53. Mirmasoomi SR, Mehdipour Ghazi M, Galedari M (2017) Photocatalytic degradation of diazinon under visible light using TiO_2/Fe_2O_3 nanocomposite synthesized by ultrasonic-assisted impregnation method. *Separation and Purification Technology 175*:418–427. https://doi.org/10.1016/j.seppur.2016.11.021
54. Mora-Gómez J, Escribá-Jiménez S, Carrillo-Abad J, et al (2022) Study of the chlorfenvinphos pesticide removal under different anodic materials and different reactor configuration. *Chemosphere 290*:133294. https://doi.org/10.1016/j.chemosphere.2021.133294
55. Mortazavian S, Saber A, James DE (2019) Optimization of photocatalytic degradation of acid blue 113 and acid red 88 textile dyes in a uv-c/tio_2 suspension system: Application of response surface methodology (RSM). *Catalysts 9*:360. https://doi.org/10.3390/catal9040360
56. Muthukumar C, Alam S, Iype E, B.g. PK (2021) Statistical analysis of photodegradation of methylene blue dye under natural sunlight. *Optical Materials 122*:111809. https://doi.org/10.1016/j.optmat.2021.111809
57. OECD (2006) Test No. 208: Terrestrial Plant Test: Seedling Emergence and Seedling Growth Test. Organisation for Economic Co-operation and Development, Paris
58. Oliveira C, Alves A, Madeira LM (2014) Treatment of water networks (waters and deposits) contaminated with chlorfenvinphos by oxidation with Fenton's reagent. *Chemical Engineering Journal 241*:190–199. https://doi.org/10.1016/j.cej.2013.12.026
59. Pandis PK, Kalogirou C, Kanellou E, et al (2022) Key points of advanced oxidation processes (AOPs) for wastewater, organic pollutants and pharmaceutical waste treatment: A mini review. *ChemEngineering 6*:8. https://doi.org/10.3390/chemengineering6010008
60. PN EN 1484 (1999) PN EN 1484 - Water analysis - Guidelines for the determination of total organic carbon (TOC) and dissolved organic carbon (DOC). https://standards.iteh.ai/catalog/standards/cen/7d0a16de-63ee-4536-a6f4-9ec990809a08/en-1484-1997. Accessed 13 Aug 2024
61. Puiu D, Galaon T, Cruceru L, et al (2017) New Study Concerning the Biodegradation of Dimethoate, Chlorpyrifos and Chlorfenvinphos in some Medicinal Plants. *Revista de Chimie 68*:1740–1743
62. Pulicharla R, Proulx F, Behmel S, et al (2020) Trends in ozonation disinfection by-products—occurrence, analysis and toxicity of carboxylic acids. *Water 12*:756. https://doi.org/10.3390/w12030756
63. Rayaroth MP, Aravindakumar CT, Shah NS, Boczkaj G (2022) Advanced oxidation processes (AOPs) based wastewater treatment - unexpected nitration side reactions - a serious environmental issue: A review. *Chemical Engineering Journal 430*:133002. https://doi.org/10.1016/j.cej.2021.133002
64. Rayaroth MP, Marchel M, Boczkaj G (2023) Advanced oxidation processes for the removal of mono

and polycyclic aromatic hydrocarbons – A review. *Science of The Total Environment 857*:159043. https://doi.org/10.1016/j.scitotenv.2022.159043

65. Rizal MY, Saleh R, Taufik A, Yin S (2021) Photocatalytic decomposition of methylene blue by persulfate-assisted Ag/Mn_3O_4 and Ag/Mn_3O_4/graphene composites and the inhibition effect of inorganic ions. *Environmental Nanotechnology, Monitoring & Management 15*:100408. https://doi.org/10.1016/j.enmm.2020.100408
66. Roselló-Márquez G, Fernández-Domene RM, García-Antón J (2021) Organophosphorus pesticides (chlorfenvinphos, phosmet and fenamiphos) photoelectrodegradation by using WO_3 nanostructures as photoanode. *Journal of Electroanalytical Chemistry 894*:115366. https://doi.org/10.1016/j.jelechem.2021.115366
67. Rueda-Márquez JJ, Levchuk I, Manzano M, Sillanpää M (2020) Toxicity reduction of industrial and municipal wastewater by advanced oxidation processes (Photo-Fenton, UVC/H_2O_2, Electro-Fenton and Galvanic Fenton): A review. *Catalysts 10*:612. https://doi.org/10.3390/catal10060612
68. Saien J, Jafari F (2022) Methods of persulfate activation for the degradation of pollutants: *Fundamentals and Influencing Parameters*. https://doi.org/10.1039/9781839166334-00001
69. Sgroi M, Anumol T, Vagliasindi FGA, et al (2021) Comparison of the new Cl_2/O_3/UV process with different ozone- and UV-based AOP's for wastewater treatment at pilot scale: Removal of pharmaceuticals and changes in fluorescing organic matter. *Science of The Total Environment 765*:142720. https://doi.org/10.1016/j.scitotenv.2020.142720
70. Sharma AK, Tiwari RK, Gaur MS (2016) Nanophotocatalytic UV degradation system for organophosphorus pesticides in water samples and analysis by Kubista model. *Arabian Journal of Chemistry 9*:S1755–S1764. https://doi.org/10.1016/j.arabjc.2012.04.044
71. Sigurnjak M, Ukić Š, Cvetnić M, et al (2020) Combined toxicities of binary mixtures of alachlor, chlorfenvinphos, diuron and isoproturon. *Chemosphere 240*:124973. https://doi.org/10.1016/j.chemosphere.2019.124973
72. Sofia DR (2020) The effect of ozonation on dissolved oxygen and microbiological content in refill drinking water. *IOP Conf Ser: Earth Environ Sci 443*:012025. https://doi.org/10.1088/1755-1315/443/1/012025
73. Sosnowska B, Huras B, Krokosz A, Bukowska B (2013) The effect of bromfenvinphos, its impurities and chlorfenvinphos on acetylcholinesterase activity. *International Journal of Biological Macromolecules 57*:38–44. https://doi.org/10.1016/j.ijbiomac.2013.02.011
74. Tongur S, Yıldız S (2021) Desalination and Water Treatment Toxicity tests using flurbiprofen, naproxen, propranolol, and carbamazepine on *Lepidium sativum*, *Daphnia magna*, and *Aliivibrio fischeri*. *Desalination and Water Treatment 221*:359–366. https://doi.org/10.5004/dwt.2021.27038
75. Xia X, Zhu F, Li J, et al (2020) A review study on sulfate-radical-based advanced oxidation processes for domestic/industrial wastewater treatment: degradation, efficiency, and mechanism. *Frontiers in Chemistry 8*.
76. Yang J, Gao Y, Song T, et al (2024) Tetracycline removal using NaIO4 activated by $MnSO_4$: Design and optimization via response surface methodology. *Water Science and Technology 89*:1082–1093. https://doi.org/10.2166/wst.2024.047
77. Žabar R, Sarakha M, Lebedev AT, et al (2016) Photochemical fate and photocatalysis of 3,5,6-trichloro-2-pyridinol, degradation product of chlorpyrifos. *Chemosphere 144*:615–620. https://doi.org/10.1016/j.chemosphere.2015.09.030
78. Zawadzki P (2019) Decolorisation of methylene blue with sodium persulfate activated with visible light in the presence of glucose and sucrose. *Water, air, and soil pollution 230*:313–313. https://doi.org/10.1007/s11270-019-4372-x
79. Zhang K, Liu M, Song X, Wang D (2023) Application of luminescent bacteria bioassay in the detection of pollutants in soil. *Sustainability 15*:7351. https://doi.org/10.3390/su15097351